

MECHANICAL RESPONSE OF OUTER FRAMES IN TUNING FORK GYROSCOPE MODEL WITH CONNECTING DIAMOND-SHAPED FRAME

Vu Van The^{1,*}, Tran Quang Dung¹, Chu Duc Trinh²

¹*Le Quy Don Technical University, Hanoi, Vietnam*

²*Vietnam National University, Hanoi, Vietnam*

*E-mail: thevutb@gmail.com

Received: 24 July 2018 / Published online: 29 October 2018

Abstract. In tuning fork micro-gyroscopes, two outer frames are connected by using the linking elements. The driving vibrations of the two outer frames are required to be exactly opposite to generate the opposite sensing modes perpendicular to driving direction. These opposite driving vibrations are provided by a mechanical structure named the diamond-shaped frame. This paper presents mechanical responses of two outer frames in a proposed model of tuning fork gyroscope when an external force with different types is applied to them. The results show that the presence of a diamond-shaped frame guarantees the absolute anti-phase mode for the driving vibrations of outer frames.

Keywords: tuning fork gyroscope; anti-phase mode; mechanical response.

1. INTRODUCTION

Gyroscopes are physical sensors that detect and measure the angle or angular velocity of an object which relatively rotates in an inertial frame of reference. The name “gyroscope” originated from a French Scientist, Léon Foucault, combining the Greek word “skopeein” meaning to see and the Greek word “gyros” meaning rotation, during his experiments to measure the rotation of the Earth [1].

Micro-Electro-Mechanical Systems (MEMSs) are devices and systems integrated with mechanical elements, sensors, actuators, and electronic circuits on a common silicon substrate through micro-fabrication technology. A normal MEMS device consists of a central unit that processes data, the microprocessor and several components that interact with the outside such as micro-sensors and micro-actuators.

MEMS Vibratory Gyroscope (MVG) is a kind of micro-sensor used to detect and determine the angular velocity or rotational angle of a body into which the MVG is integrated. The operation of this micro-sensor is based on the Coriolis principle to transfer energy from the primary vibration to a secondary one [1–3]. MVGs have been extensively applied in automotive and aerospace industries and consumer electronics market

given notable advantages including marked reduction in cost, size, and weight. Indeed, previous researches into vibrational characteristics of the proof-mass in gyroscopes have shown that the MVGs have many advantages over traditional gyroscopes for their small size, low power consumption, low cost, batch fabrication and high performance [1–7].

The MEMS tuning fork gyroscope (TFG), which consists of two identical tines vibrating in opposite direction (anti-phase), is a widely used class of MVG. The advantage of the tuning fork structure is the high resistance to the exciting phase deviation in operating [4–6]. However, the traditional MEMS tuning fork structure with the direct mechanical coupling between two tines likely causes an in-phase vibratory mode [6]. Therefore, it is necessary to design a novel TFG with a mechanism indirectly connecting two tines to create an anti-phase state, where connecting mechanism plays an important role for resisting phase deviation of two tines [7–9]. This mechanism is termed diamond-shaped frame, and its detailed description can be found elsewhere [10].

This paper focuses on setting up differential equations of motion and studying the vibrations of two outer frames when they are connected indirectly by a diamond-shaped frame. These outer frames are expected to vibrate with the absolute anti-phase mode to create the anti-phase mode for sensing vibrations of proof-masses in proposed TFG model.

2. CONFIGURATION OF THE PROPOSED TFG

The proposed model consists of two identical tines as shown in Fig. 1. Each tine is defined as a single gyroscope and includes a proof-mass (1) and an outer frame (2). The configuration and dynamic characteristics of each single gyroscope are provided in [11]. This outer frame is connected to the proof-mass by four elastic beams (3) and suspended on substrate thanks to four other elastic beams (4). Each of these beams is linked to the substrate (not be presented in Fig. 1) by an anchor (5) to allow the outer frame and the proof-mass to move freely in two perpendicular directions. Two single gyroscopes are connected through a diamond-shaped frame to create the proposed TFG. This frame has four rigid bars (7) with length L and the rectangular cross-section $b \times h$, where h and b are the thickness and width of each bar, respectively. The bars are connected to the connectors by elastic stems (8) with the width s ($s < b$). The configuration and dynamics analysis of this frame was carried out in our previous research [10].

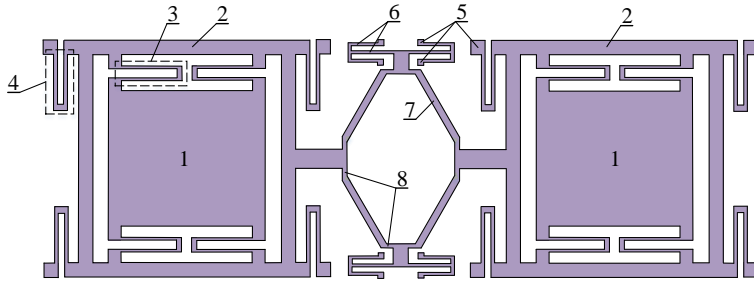


Fig. 1. 3D model of the proposed TFG with diamond-shaped frame

Fig. 2 describes a physical model of this TFG, where k_{x1} , k_{x2} , k_{y1} , and k_{y2} are the equivalent stiffness of the elastic beams; c_{x1} , c_{x2} , c_{y1} , and c_{y2} are damping coefficients in x - and y -direction; m_{S1} and m_{S2} are values of the proof-masses; and m_{f1} and m_{f2} are masses of the outer frames. The points (e.g. A, B, C, and D) are the nodes of the diamond-shaped frame.

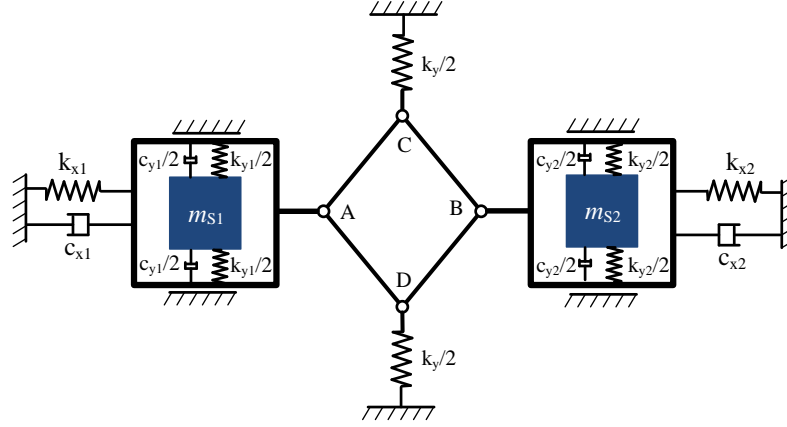


Fig. 2. Physical model of the TFG

3. DIFFERENTIAL EQUATIONS OF MOTION

The four beams of the diamond-shaped frame are assumed to be absolutely rigid. The displacement at the end of the beams (A, B, C, and D) is carried out by the elasticity of stems with the smaller section. When the diamond-shaped frame links two single gyroscopes to create tuning fork structure, points A and B only displace in x -direction and points C and D only do in y -direction. The displacement of point A is x_1 , while point C displaces y_1 from the initial position. Points B and D are the same displacements with A and C except for the direction of motion (Fig. 3(a)). These displacements depend mutually and have a relation as follows

$$\begin{aligned} y_1 &= \sqrt{L^2 - (L_1 - x_1)^2} - L_2, \\ y_2 &= \sqrt{L^2 - (L_1 - x_2)^2} - L_2, \end{aligned} \quad (1)$$

where $L_1 = L \cos \alpha_0$, $L_2 = L \sin \alpha_0$, and α_0 is the angle to define initial position of rigid bars of the diamond-shaped frame.

Thence the elastic forces are defined by the followed expressions

$$F_{Dy} = k_y y_D / 2 = k_y y_1 / 2, \quad (2)$$

$$F_{Cy} = k_y y_C / 2 = k_y y_2 / 2. \quad (3)$$

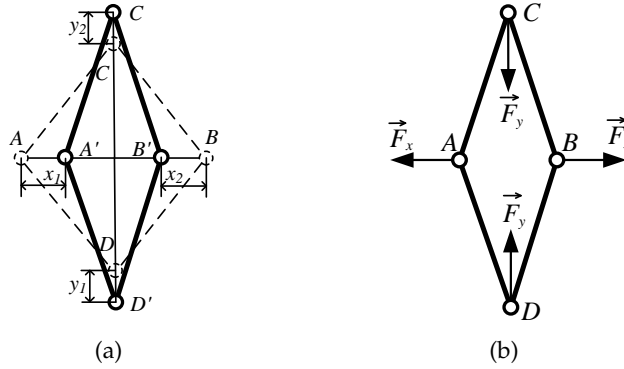


Fig. 3. Schema of deformation (a) and elastic forces (b) of diamond-shaped frame

The elastic force applied to the outer frames in x -direction is determined as the followed expression

$$F_x = \frac{1}{2}(F_{Cy} + F_{Dy})\cot\alpha, \quad (4)$$

with α is an angular rotation of a rigid beam when diamond-shaped frame operated.

The Eq. (4) describes the relation between elastic forces in y -direction and the corresponding force in x -direction.

In this issue, both outer frame and proof-mass vibrate in the driving direction. In essence, they are considered as one element with total mass m_1 and m_2 , respectively ($m_i = m_{fi} + m_{si}$). The component forces applying to the masses m_1 and m_2 are shown in Fig. 4 after splitting them.

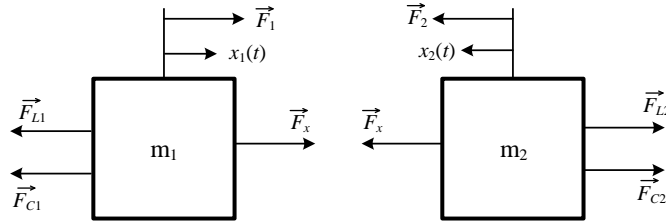


Fig. 4. The forces applied to the outer frames

In Fig. 4, \vec{F}_1 and \vec{F}_2 are external forces applied to the outer frames; \vec{F}_{L1} and \vec{F}_{L2} are elastic forces of elastic beams with the stiffness coefficients k_{x1} and k_{x2} respectively; \vec{F}_{C1} and \vec{F}_{C2} are damping forces with damping coefficients c_{x1} and c_{x2} known as the slide air damping between the masses and the substrate, and \vec{F}_x is elastic force mentioned above.

$$F_{L1} = k_{x1}x_1; \quad F_{L2} = k_{x2}x_2, \quad (5)$$

$$F_{C1} = c_{x1}\dot{x}_1; \quad F_{C2} = c_{x2}\dot{x}_2. \quad (6)$$

By using the second Newton law, the motion differential equations for the system are obtained as follows

$$\begin{aligned} m_1 \ddot{x}_1 &= \vec{F}_{L1} + \vec{F}_{C1} + \vec{F}_x + \vec{F}_1, \\ m_2 \ddot{x}_2 &= \vec{F}_{L2} + \vec{F}_{C2} + \vec{F}_x + \vec{F}_2. \end{aligned} \quad (7)$$

Eqs. (7) are expanded as

$$\begin{aligned} m_1 \ddot{x}_1 + c_{x1} \dot{x}_1 + k_{x1} x_1 + \frac{1}{4} k_y (y_1 + y_2) \cot \alpha &= F_1, \\ m_2 \ddot{x}_2 + c_{x2} \dot{x}_2 + k_{x2} x_2 + \frac{1}{4} k_y (y_1 + y_2) \cot \alpha &= F_2. \end{aligned} \quad (8)$$

Adding some equations describing the geometric relations between the displacements x_1 , x_2 and y_1 , y_2

$$\begin{aligned} L_1 &= L \cos \alpha_0; \quad L_2 = L \sin \alpha_0, \\ y_1 &= \sqrt{L^2 - (L_1 - x_1)^2} - L_2, \\ y_2 &= \sqrt{L^2 - (L_1 - x_2)^2} - L_2, \\ \alpha &= \arctg \left(\frac{y_1}{x_1} \right). \end{aligned} \quad (9)$$

The differential equations of motion for the system with displacements in x -direction become

$$\begin{aligned} m_1 \ddot{x}_1 + c_{x1} \dot{x}_1 + k_{x1} x_1 + \frac{1}{4} k_y \left(\sqrt{L^2 - (L_1 - x_1)^2} + \sqrt{L^2 - (L_1 - x_2)^2} - 2L_2 \right) \cot \alpha &= F_1, \\ m_2 \ddot{x}_2 + c_{x2} \dot{x}_2 + k_{x2} x_2 + \frac{1}{4} k_y \left(\sqrt{L^2 - (L_1 - x_1)^2} + \sqrt{L^2 - (L_1 - x_2)^2} - 2L_2 \right) \cot \alpha &= F_2, \\ L_1 &= L \cos \alpha_0, \\ L_2 &= L \sin \alpha_0, \\ \alpha &= \operatorname{atan} \left(\frac{\sqrt{L^2 - (L_1 - x_1)^2} - L_2}{x_1} \right). \end{aligned} \quad (10)$$

4. VIBRATIONAL CHARACTERISTICS OF TWO OUTER FRAMES

The result of the vibratory problem is received by using Matlab software with suitable initial parameters. In this paper, the research cases consist of: free vibration; forced vibration with harmonic impulse form. The characteristic parameters of the TFG system are shown in Tab. 1.

4.1. Free vibration

In order to demonstrate the ability to vibrate in x -direction, a study on free vibration of the system is carried out firstly. When the system has no exciting force and the initial parameters are: $x_1 = 2.5 \times 10^{-5}$ m, $x_2 = 2.5 \times 10^{-5}$ m, the free vibration of two element masses is showed in Fig. 5.

The results show that the outer frames are able to oppositely vibrate in the driving direction. Their amplitude seems like a constant in a short time. However, the air damping

Table 1. The parameters of the TFG

Parameter	Value	Unit
Mass of the left single gyroscope: m_1	2.65×10^{-7}	kg
Mass of the right single gyroscope: m_2	2.65×10^{-7}	kg
Driving stiffness of the left single gyroscope: k_{x_1}	25.2	N/m
Driving stiffness of the right single gyroscope: k_{x_2}	25.2	N/m
Damping coefficient in left drive direction: c_{x_1}	2×10^{-5}	kg/s
Damping coefficient in right drive direction: c_{x_2}	2×10^{-5}	kg/s
Stiffness of diamond-shaped frame in y -direction: k_y	10	N/m
Length of a rigid bar: L	10^{-4}	m
Initial angle of rigid bar: α_0	60°	degree

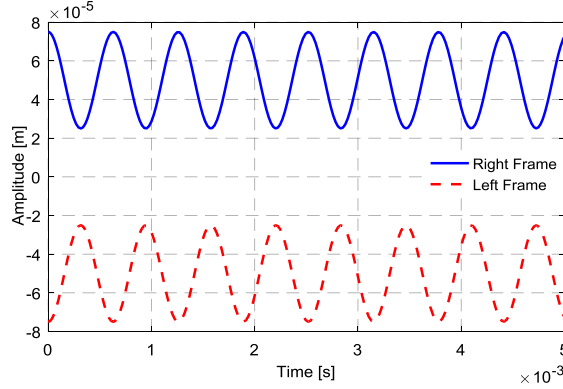


Fig. 5. The free vibration of two outer frames

causes decreasing slowly in amplitude to time. Two elements vibrate around equilibrium position ($\pm 5 \times 10^{-5}$ m) with decreased amplitude after every period (initial amplitude 2.5×10^{-5} m). These vibrations are symmetric through the centre of the diamond-shaped frame.

4.2. Force vibration

When applying two external forces to the outer frames with a constant value (3×10^{-4} N) and their direction from the centre of the diamond-shaped frame to each outer frame, these outer frames vibrate from their equilibrium position ($\pm 5 \times 10^{-5}$ m) and outward from the centre (Fig. 6(a)). While vibrations of them are anti-phase mode when applied forces with opposite direction toward to the centre (Fig. 6(b)). The amplitudes in both cases of external forces are the same value ($23 \mu\text{m}$).

According to the results in Fig. 6, the vibrational amplitude appears as constant through some continuous periods. These vibrations still guarantee anti-phase mode and symmetry through the centre of the diamond-shaped frame.

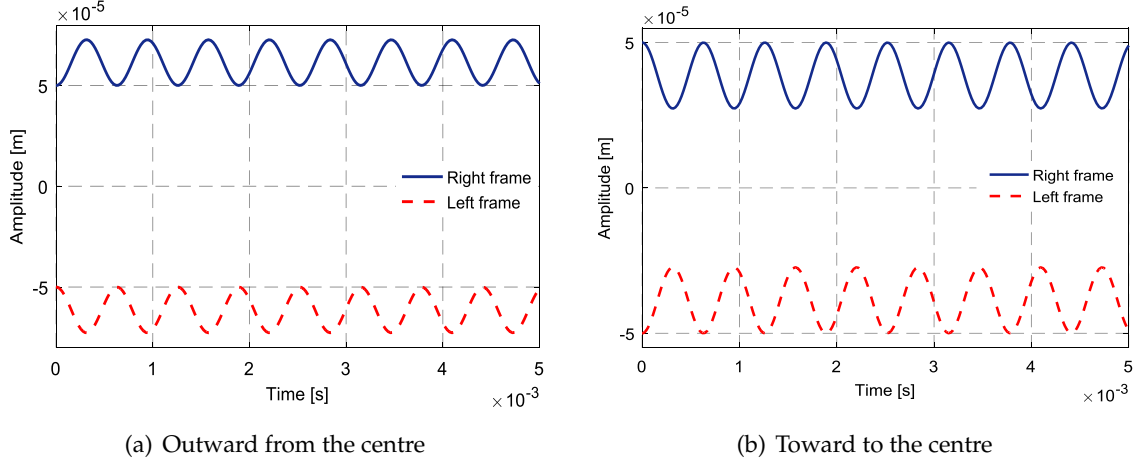


Fig. 6. Vibration of outer frames with constant external force

The relation between the vibratory amplitude and the force value in case of changing the value of k_y is shown in Fig. 7. The displacements of outer frames in driving direction should be smaller than 3×10^{-5} m, hence the value of exciting force should be smaller than 4×10^{-4} N (Fig. 7).

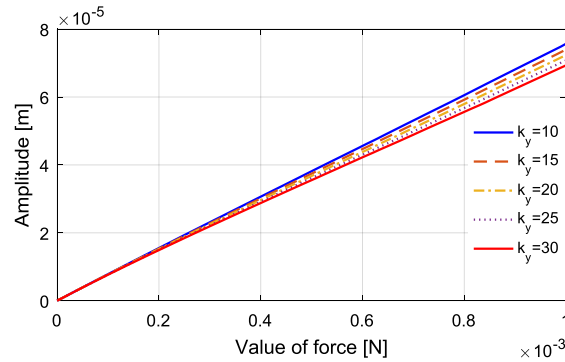


Fig. 7. Relation between vibrational amplitude and value of external force

The exciting harmonic force applied to outer frames should have a form as follows

$$F_1 = F_0 \sin 2\pi ft; \quad F_2 = F_0 \sin(2\pi ft + \pi). \quad (11)$$

Function (11) is defined by the force value F_0 and the exciting frequency f . These parameters are determined by analyzing the amplitude - frequency response of the system. To reduce the time of the calculation and guarantee the efficiency, the exciting frequency of the system is assessed from 1400 Hz to 1800 Hz (Fig. 8(a)). According to the result shown in Fig. 8(a), the exciting frequency should be 1590 Hz. With this frequency, the

amplitude of driving vibration depends on the value of F_0 . To match with the configuration of the diamond-shaped frame presented in [10] (i.e. less than $30 \mu\text{m}$), the value of exciting force should be chosen as $1 \div 6 \mu\text{N}$ (Fig. 8(b)). In case of the larger exciting force, the vibrational output increases drastically, and unexpected vibration will appear.

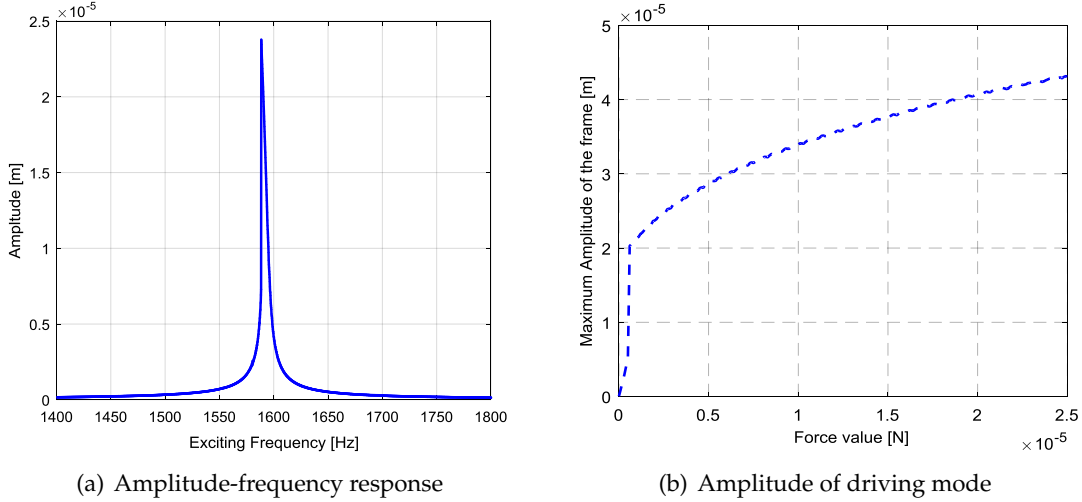


Fig. 8. Determining the exciting frequency and value of force

When applying the exciting forces with the above function (11) to two outer frames, their stable vibrations in driving direction are similar to harmonic form as shown in Fig. 9. Due to the absolutely opposite direction of two exciting forces, the anti-phase mode of these vibrations is assured completely. Therefore, the anti-phase mode for sensing vibrations of two proof-masses is created in two single gyroscopes of TFG model mentioned above.

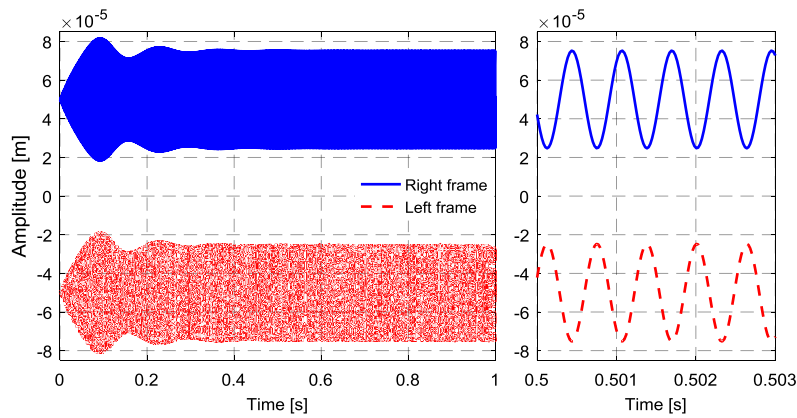


Fig. 9. Vibration of driving mode with harmonic exciting force

5. CONCLUSION

The paper introduces the TFG model with a connecting frame named diamond-shaped frame to directly link two single gyroscopes in two sides of this frame. The differential equations of motion of two outer frames in every single gyroscope are set up following the second Newton law. By using Matlab software, the vibrational form of two outer frames in some different cases is studied to demonstrate that the driving vibration of these frames is completely opposite thanks to the diamond-shaped frame. These results show that the presence of the diamond-shaped frame guarantees the absolute anti-phase mode for the driving vibrations of outer frames. They are the important basis for further researches into the sensing mode in proposed TFG for purpose of increasing the performance of the sensor.

REFERENCES

- [1] C. Acar and A. Shkel. *MEMS vibratory gyroscopes: structural approaches to improve robustness*. Springer Science & Business Media, (2008).
- [2] A. M. Shkel, R. Horowitz, A. A. Seshia, S. Park, and R. T. Howe. Dynamics and control of micromachined gyroscopes. In *Proceedings of the American Control Conference, IEEE, IEEE*, Vol. 3, (1999), pp. 2119–2124.
- [3] W. Yongpeng and S. Huilin. Modeling and simulation for a vibratory tuning-fork MEMS gyroscope. In *Third International Conference on Measuring Technology and Mechatronics Automation (ICMTMA), IEEE, IEEE*, Vol. 2, (2011), pp. 605–608.
- [4] V. Apostolyuk and F. E. H. Tay. Dynamics of micromechanical Coriolis vibratory gyroscopes. *Sensor Letters*, **2**, (3-4), (2004), pp. 252–259. <https://doi.org/10.1166/sl.2004.057>.
- [5] B. Choi, S. Y. Lee, T. Kim, and S. S. Baek. Dynamic characteristics of vertically coupled structures and the design of a decoupled micro gyroscope. *Sensors*, **8**, (6), (2008), pp. 3706–3718. <https://doi.org/10.3390/s8063706>.
- [6] Y. Guan, S. Gao, L. Jin, and L. Cao. Design and vibration sensitivity of a MEMS tuning fork gyroscope with anchored coupling mechanism. *Microsystem Technologies*, **22**, (2), (2016), pp. 247–254. <https://doi.org/10.1007/s00542-014-2405-3>.
- [7] Y. Guan, S. Gao, H. Liu, L. Jin, and S. Niu. Design and vibration sensitivity analysis of a MEMS tuning fork gyroscope with an anchored diamond coupling mechanism. *Sensors*, **16**, (4), (2016). <https://doi.org/10.3390/s16040468>.
- [8] T. Q. Trinh, L. Q. Nguyen, D. V. Dao, H. M. Chu, and H. N. Vu. Design and analysis of a z-axis tuning fork gyroscope with guided-mechanical coupling. *Microsystem Technologies*, **20**, (2), (2014), pp. 281–289. <https://doi.org/10.1007/s00542-013-1947-0>.
- [9] M. N. Nguyen, N. S. Ha, L. Q. Nguyen, H. M. Chu, and H. N. Vu. Z-axis micro-machined tuning fork gyroscope with low air damping. *Micromachines*, **8**, (2), (2017). <https://doi.org/10.3390/mi8020042>.
- [10] V. V. The, T. Q. Dung, V. M. Hoan, and C. D. Trinh. Studying of dynamic response of a diamond-shaped micro silicon frame. *Journal of Science and Technique, Military Technical Academy*, **186**, (2017), pp. 34–42.
- [11] V. V. The, T. Q. Dung, and C. D. Trinh. Dynamic analysis of a single MEMS vibratory gyroscope with decoupling connection between driving frame and sensing proof mass. *International Journal of Applied Engineering Research*, **13**, (7), (2018), pp. 5554–5561.